Quantum Jumps of the Micromaser Field: Dynamic Behavior Close to Phase Transition Points

O. Benson, G. Raithel, and H. Walther
Max-Planck-Institut für Quantenoptik and Sektion Physik der Universität München, D-85748 Garching, Federal Republic of Germany
(Received 24 January 1994)

The field of the one-atom maser, or micromaser, shows strong variations in certain parameter regions usually identified as phase transitions. In this paper the time development of the field in the vicinity of those regions is investigated. Depending on the parameters, spontaneous jumps or slow transitions between two metastable field values can be observed. Hysteresis behavior also occurs. The results are explained by means of a quantum Monte Carlo simulation of the maser field as well as a Fokker-Planck description used earlier in micromaser theory.

PACS numbers: 42.52.+x, 32.80.−t, 42.50.Lc

The one-atom maser, or micromaser, is a pure quantum device operating with only a few photons and less than one pump atom on the average in the maser cavity [1,2]. It is thus an ideal device to study quantum phenomena in radiation-atom interaction. One mode of the superconducting niobium cavity is tuned to a transition between highly excited states (Rydberg states) of the rubidium atom. The cavity field is pumped by a beam of velocity-selected Rydberg atoms entering the cavity in the upper maser level. The pumping occurs via the interaction of single atoms with the cavity field. The dynamics of this interaction has features which are purely quantum, such as collapse and revival in the Rabi flopping process [2,3]. Furthermore, the photon statistics of the micromaser field can be sub-Poissonian [4,5] and a two-photon maser is feasible also [6].

Under steady-state conditions, the photon statistics $P(n)$ of the field is essentially determined by the pump parameter, $\Theta = N_{\rm ex}^{1/2}\Omega t_{\rm int}/2$ [7,8]. Here, $N_{\rm ex}$ is the average number of atoms that enter the cavity during $\tau_{\rm cav}$, Ω the vacuum Rabi flopping frequency, and $t_{\rm int}$ is the atom-cavity interaction time. The quantity $\langle\nu\rangle = \langle n\rangle/N_{\rm ex}$ shows the following generic behavior (see Fig. 1): It suddenly increases at the maser threshold value $\Theta = 1$, and reaches a maximum for $\Theta \approx 2$ (denoted by A in Fig. 1). The maser threshold shows the characteristics of a continuous phase transition [7]. As Θ further increases, $\langle\nu\rangle$ decreases and reaches a minimum at $\Theta \approx 2\pi$, and then abruptly increases to a second maximum (B in Fig. 1). This general type of behavior recurs roughly at integer multiples of 2π, but becomes less pronounced with increasing Θ. The reason for the periodic maxima of $\langle\nu\rangle$ is that for integer multiples of $\Theta = 2\pi$ the pump atoms perform an almost integer number of full Rabi flopping cycles, and start to flip over at a slightly larger value of Θ, thus leading to enhanced photon emission. The periodic maxima in $\langle\nu\rangle$ for $\Theta = 2\pi, 4\pi, \ldots$ can be interpreted as first-order phase transitions [7]. The field strongly fluctuates for all phase transitions (A, B, and C in Fig. 1), the large photon number fluctuations for $\Theta \approx 2\pi$ and multiples thereof being caused by the presence of two maxima in the photon number distribution $P(n)$ at photon numbers n_l and n_h ($n_l < n_h$). For n_l and n_h the atoms perform almost integer numbers m or $m+1$ of full Rabi flopping cycles, respectively. If the pump parameter is scanned across $\Theta \approx m2\pi$, the maximum of $P(n)$ at n_l completely dies out, and is replaced by the new peak at the higher photon number n_h. For $\Theta = m2\pi$, the simultaneous presence of two maxima of $P(n)$ leads to spontaneous jumps of the micromaser field between two average photon numbers n_l and n_h.

The phenomenon of the two coexisting maxima in $P(n)$ was also studied in a semiheuristic Fokker-Planck (FP) approach [7]. There, the photon number distribution $P(n)$ is replaced by a probability function $P(\nu,\tau)$ with continuous variables $\tau = t/\tau_{\rm cav}$ and $\nu(n) = n/N_{\rm ex}$, the latter replacing the photon number n. The steady-state solution obtained for $P(\nu,\tau)$, $\tau \gg 1$, can be constructed by means of an effective potential $V(\nu)$ showing minima

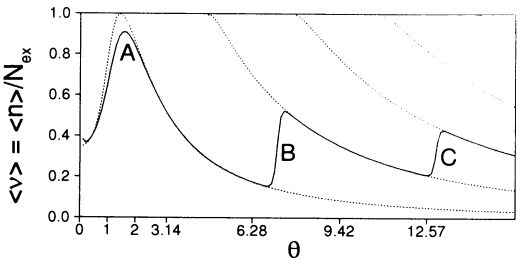

FIG. 1. Mean value of $\nu = n/N_{\rm ex}$ versus the pump parameter $\Theta = \Omega t_{\rm int}\sqrt{N_{\rm ex}}/2$, where the value of Θ is changed via $N_{\rm ex}$. The solid line represents the micromaser solution for $\Omega = 36$ kHz, $t_{\rm int} = 35$ μs, and temperature $T = 0.15$ K. The dotted lines are semiclassical steady-state solutions corresponding to fixed stable gain=loss equilibrium photon numbers [9]. The crossing points between a line $\Theta = \text{const}$ and the dotted lines correspond to the values where minima in the Fokker-Planck potential $V(\nu)$ occur. The phase transition B is investigated in the experiments displayed in Figs. 4 and 6, whereas the experiments shown in Figs. 3 and 5 are related to C.

0031-9007/94/72(22)/3506(4)$06.00

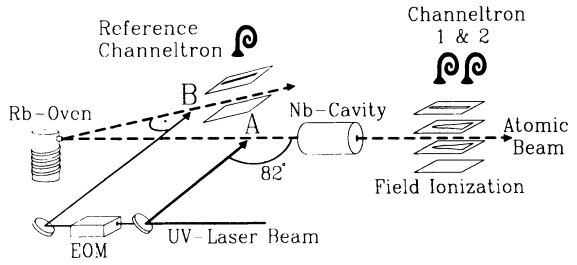

FIG. 2. Sketch of the experimental setup. The rubidium atoms emerge from an atomic beam oven and are excited at an angle of 82° at location A. After interaction with the cavity field, they enter a state-selective field ionization region, where channeltrons 1 and 2 detect atoms in the upper and lower maser levels, respectively. A small fraction of the UV radiation passes through an electro-optic modulator (EOM), which generates sidebands of the UV radiation. The blueshifted sideband is used to stabilize the frequency of the laser onto the Doppler-free resonance monitored with a secondary atomic beam produced by the same oven (location B).

at positions where maxima of $P(\nu,\tau)$, $\tau \gg 1$, are found. Close to $\Theta = 2\pi$ and multiples thereof, the effective potential $V(\nu)$ exhibits two equally attractive minima located at stable gain-loss equilibrium points of maser operation [9] (see Fig. 1). The mechanism at the phase transitions mentioned is always the same: A minimum of $V(\nu)$ loses its global character when Θ is increased, and is replaced in this role by the next one. This reasoning is a variation of the Landau theory of first-order phase transitions, with $\sqrt{\nu}$ being the order parameter. This analogy actually leads to the notion that in the limit $N_{\rm ex} \to \infty$ the change of the micromaser field around integer multiples of $\Theta = 2\pi$ can be interpreted as first-order phase transitions.

Close to first-order phase transitions long field evolution time constants $\tau_{\rm field}$ are expected [7]. This phenomenon is experimentally demonstrated in this paper, as well as related phenomena, such as spontaneous quantum jumps between equally attractive minima of $V(\nu)$, bistability, and hysteresis. Some of those phenomena are also predicted in the two-photon micromaser [6], for which qualitative evidence of first-order phase transitions and hysteresis is reported in [10,11].

The experimental setup used is shown in Fig. 2. It is similar to that described in [4,5]. As before, ^{85}Rb atoms were used to pump the maser. They are excited from the $5S_{1/2}, F = 3$ ground state to $63P_{3/2}, m_J = \pm\frac{1}{2}$ states by linearly polarized light of a frequency-doubled c.w. ring dye laser. The polarization of the laser light is linear and parallel to the likewise linearly polarized maser field, and therefore only $\Delta m_J = 0$ transitions are excited. Superconducting niobium cavities resonant with the transition to the $61D_{3/2}, m_J = \pm\frac{1}{2}$ states were used; the corresponding resonance frequency is 21.506 GHz. The experiments were performed in a ^{3}He/^{4}He dilution refrigerator with cavity temperatures $T \approx 0.15$ K. The cavity Q values ranged from 4×10^9 to 8×10^9. The

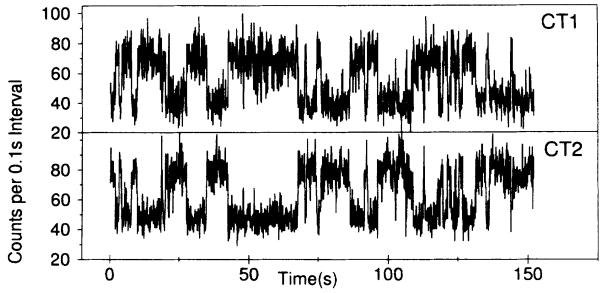

FIG. 3. Quantum jumps between two equally stable operation points of the maser field. The channeltron counts are plotted versus time (CT1 = upper state; CT2 = lower state).

velocity of the Rydberg atoms and thus their interaction time $t_{\rm int}$ with the cavity field were preselected by exciting a particular velocity subgroup with the laser. For this purpose, the laser beam irradiated the atomic beam at an angle of approximately 82°. As a consequence, the UV laser light (linewidth ≈ 2 MHz) is blueshifted by 50–200 MHz by the Doppler effect, depending on the velocity of the atoms.

Information on the maser field and interaction of the atoms in the cavity can be obtained solely by state-selective field ionization of the atoms in the upper or lower maser level after they have passed through the cavity. The field ionization detector was recently modified, so that there is now a detection efficiency of $\eta = (35 \pm 5)\%$. For different $t_{\rm int}$ the atomic inversion has been measured as a function of the pump rate. By comparing the results with micromaser theory [7], the coupling constant Ω is found to be $\Omega = (40 \pm 10)\,\frac{rd}{s}$.

Depending on the parameter range, essentially three regimes of the field evolution time constant $\tau_{\rm field}$ can be distinguished. First we discuss the results for intermediate time constants. The maser was operated under steady-state conditions close to the second first-order phase transition (C in Fig. 1). The interaction time was $t_{\rm int} = 47\,\mu$s and the cavity decay time $t_{\rm cav} = 60$ ms. The value of $N_{\rm ex}$ necessary to reach the second first-order phase transition was $N_{\rm ex} \approx 200$. For these parameters, the two maxima in $P(n)$ are manifested in spontaneous jumps of the maser field between the two maxima with a time constant of ≈ 5 s. This fact and the relatively large pump rate led to the clearly observable field jumps shown in Fig. 3. Because of the large cavity field decay time, the average number of atoms in the cavity was still as low as 0.17. The two discrete values for the counting rates correspond to the metastable operating points of the maser, which correspond to $\approx$70 and $\approx$140 photons. In the FP description, the two values correspond to two equally attractive minima in the FP potential $V(\nu)$. If one considers, for instance, the counting rate of lower-state atoms (CT2 in Fig. 3), the lower (higher) plateaus correspond to time intervals in the low (high) field metastable operating point. If the actual photon number distribution is averaged over a time interval containing many spon-

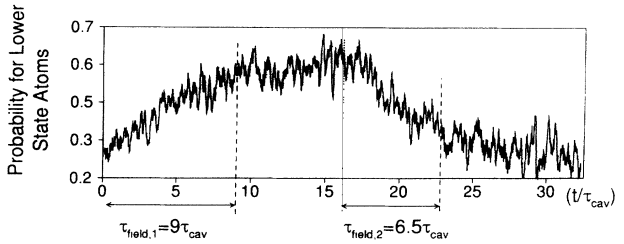

FIG. 4. Measurements at low atomic flux. By switching the UV laser intensity the pump rate was periodically changed back and forth across phase transition B (see Fig. 1). The counting events in the channeltrons were recorded as a function of time modulo the cycle period. The resulting probability for lower-state atoms is plotted versus time. The experiment was performed with an average value of $N_{ex} \approx 30$, $t_{int} = 47$ μs, and $\tau_{cav} = 60$ ms. The long evolution time constants $\tau_{field,i} \approx 8\tau_{cav}$ can be clearly identified.

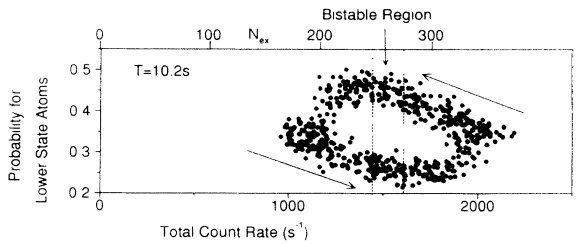

FIG. 5. Hysteresis cycle of the micromaser observed with $t_{int} = 35$ μs and $t_{cav} = 60$ ms. The cycle period was $T = 10.2$ s. In the central part of the cycle the system is actually bistable; i.e., no spontaneous jumps between the two branches could be observed.

taneous field jumps, the steady-state result $P(n)$ of the micromaser theory is recovered.

In a parameter range where switching occurs much faster than in the case shown in Fig. 3, the individual jumps cannot be resolved any more owing to the reduced N_{ex} necessary in this case. Therefore, a different procedure has to be chosen for the investigation. The maser pump rate N_{ex} is periodically switched between two values differing by about 30% of their mean value. The individual values correspond to pump parameters Θ slightly below and above a first-order phase transition. The corresponding FP potential $V(\nu)$ has two minima at both values of Θ, the switching of Θ causing the first or the second to be the globally more stable one. In Fig. 4, N_{ex} was switched between ≈ 35 and ≈ 25 with a period of 2 s ($= 33\tau_{cav}$, corresponding to the full time scale of Fig. 4). $N_{ex} = 35$ (25) corresponds to 0.027 (0.020) atoms on the average in the cavity. The experiment runs over many switching cycles. The time is measured modulo the switching period; i.e., the time is reset to zero whenever N_{ex} is switched from the lower to the larger value. In the experiment the signal transients are averaged over many measuring periods, and hence in this case the *ensemble average* is obtained. After the switching instants, the evolution of the average signal is dominated by an exponential approach to the new steady-state values, which correspond to mean photon numbers of roughly 21 and 6. Figure 4 clearly displays the long evolution time constants τ_{field}. It is expected from theory that τ_{field} rapidly increases as N_{ex} is increased. This has been confirmed by a series of other measurements. Time constants of the order of $\tau_{field} \approx 5\tau_{cav}$ were obtained with $N_{ex} \approx 19$, in which case the metastable operating points of the maser differ by only ≈ 7 photons.

The third situation arises when the switching time constant becomes much longer still than in the measurement shown in Fig. 3. By using fast atoms with an interaction time of 35 μs and operating the maser at the second first-order phase transition (C in Fig. 1), it was possible to increase τ_{field} up to very long values (of the order of 15 min). In this case, a bistable cavity QED system with low photon and atom number is realized. The bistability is shown in Fig. 5, where the (detected) pump rate was linearly varied between 1000 s^{-1} and 2000 s^{-1}. Figure 5 clearly exhibits a nice hysteresis cycle (note the large value of the cycle period, $T = 10.2$ s). The width of the hysteresis region is considerable and corresponds to a change in the pump rate of 800 s^{-1}. In the bistable region, the maser can be prepared in either the upper or lower branch of the hysteresis loop. The number of photons in the cavity was $\approx 80\,(160)$ in the lower (upper) field state, and the average number of pump atoms in the cavity 0.15.

According to theoretical expectation, the area of the hysteresis cycle can be increased by scanning the pump rate more rapidly. This experiment was performed at the first first-order phase transition, corresponding to location B in Fig. 1. Owing to the comparatively small spontaneous hopping time constant of ≈ 1 s, the hysteresis cycle had to be scanned quite fast. The result is shown in Fig. 6. It can be clearly recognized that with increasing scan velocity larger parts of the metastable but globally unstable branches can be mapped out.

The experimental results can be compared to "quantum Monte Carlo" simulations of the micromaser [5,12,13]. The calculations show that even after a steady state is reached, the actual field state can strongly deviate from the temporal or ensemble average. This is most striking on the first-order phase transitions: The temporal average of the photon number distribution exhibits the discussed pair of maxima, whereas the time-dependent photon number distribution of the quantum Monte Carlo calculation performs statistical jumps between two situations where one of the two maxima dominates. This had been already predicted earlier [12]. The characteristic "hopping time" between the two situations equals the evolution time constant τ_{field} of the ensemble-averaged evolution. The values of τ_{field} are determined by computer experiments similar to those shown in Figs. 3 and 4. In the simulations, the experimental broadening of the velocity distribution and the spontaneous decay of the Rydberg atoms (lifetime ≈ 350 μs) were taken into

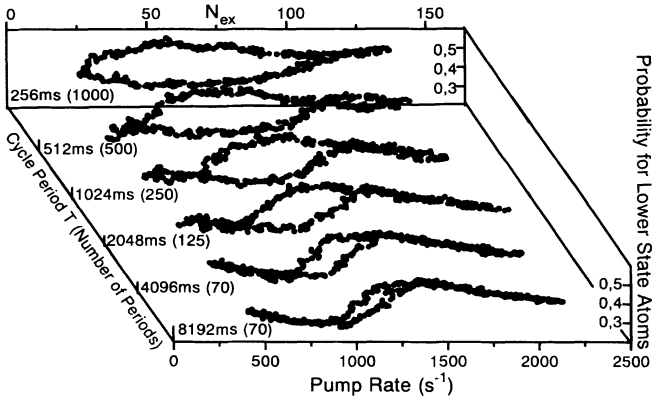

FIG. 6. Time dependence of the hysteresis cycle observed with $t_{\rm int} = 35$ μs, $t_{\rm cav} = 23$ ms, and cycle periods T. The number of recorded cycles is indicated in parentheses.

account. In all cases, the theoretical value for the hopping time was several orders of magnitude too large.

Alternatively, the results are discussed on the basis of the FP approach, which represents a good approximation of the maser dynamics if $n \gg 1$ and $\Omega t_{\rm int} \ll \sqrt{n}$ [7]. In our experiments, these conditions are reasonably well satisfied. By analogy with the experiment, we consider situations in which the effective potential $V(\nu)$ exhibits two equally attractive minima. The hopping time $\tau_{\rm field}$ between these minima is calculated by Kramers' analysis [7]. In all cases investigated, the hopping times obtained by the FP calculations and Monte Carlo simulations agree, but are significantly larger than the experimental values.

In this context it is important to note that the experiment deviates from the ideal situation treated in [7]. Any kind of additional randomness included in the theoretical model flattens the effective potential $V(\nu)$ and leads to larger hopping rates. It can be excluded that laser or atomic beam intensity fluctuations modify the experimental results. The laser intensity was stabilized, and the flux of Rydberg atoms displays ideal Poissonian statistics. In a heuristic way, we can account for all unknown fluctuations by assuming a Gaussian distribution for Ω with relative r.m.s. deviation $\delta = \langle\Omega\rangle/\Omega$, where $\langle\Omega\rangle$ is the root mean square. In order to achieve a quantitative agreement between theoretical and experimental values of the hopping rates $\delta = (15 \pm 1)\%$ has to be assumed at the first first-order phase transition point, and $\delta = (9 \pm 1)\%$ at the second. Other experimental investigations, not discussed in detail here, using a cavity resonant with the $63P_{3/2} - 61D_{5/2}$ transition, operated at the second first-order phase transition, can be reproduced by assuming $\delta = (7 \pm 2)\%$. In the following we discuss the most obvious phenomena leading to $\delta \neq 0$. Unfortunately it is not possible in the experiment to determine their relative contribution.

Stray electric fields in the holes through which the atoms enter the cavity could lead to adiabatic transitions between the magnetic sublevels. The maser would then be pumped by a mixture of magnetic sublevels, which have different atom-field couplings. Another source of perturbation may be stray electric fields in the interior of the cavity. An estimate on this phenomenon we can get from the 25 ± 5 kHz FWHM width of the maser resonance at low atomic flux, being larger than the expected value of 13 kHz. If the broadening is totally attributed to inhomogeneous electric stray fields, this results in an upper limit of ≈ 5 mV/cm. As a consequence, different Rydberg atoms experience slightly different electric stray fields, leading to a spread in the Rabi flopping frequencies and amplitudes. The Rabi flopping is less affected by intracavity stray electric fields if a large number of photons are present. This may explain that the above mentioned values of δ are smaller for higher photon numbers. Finally, fluctuations in the effective Rabi frequency may also occur when two atoms are simultaneously in the cavity; there is a small probability that this may happen in some of the described experiments.

In this work, bistability, hysteresis, and spontaneous field jumps in a micromaser have been experimentally demonstrated. The phenomenology is in excellent agreement with the micromaser theory. However, the extreme sensitivity of the Rydberg atoms to perturbing influences such as stray fields or other imperfections of the experimental setup prevent us from achieving full quantitative agreement with theory.

[1] D. Meschede, H. Walther, and G. Müller, Phys. Rev. Lett. **54**, 551 (1985).
[2] G. Rempe, H. Walther, and N. Klein, Phys. Rev. Lett. **58**, 353 (1987).
[3] J. H. Eberly, N. B. Narozhny, and J. J. Sanchez-Mondragon, Phys. Rev. Lett. **44**, 1323 (1980).
[4] G. Rempe, F. Schmidt-Kaler, and H. Walther, Phys. Rev. Lett. **64**, 2783 (1990).
[5] G. Rempe and H. Walther, Phys. Rev. A **42**, 1650 (1990).
[6] L. Davidovich, J. M. Raimond, M. Brune, and S. Haroche, Phys. Rev. A **36**, 3771 (1987); M. Brune, J. M. Raimond, P. Goy, L. Davidovich, and S. Haroche, Phys. Rev. Lett. **59**, 1899 (1987).
[7] P. Filipowicz, J. Javanainen, and P. Meystre, Phys. Rev. A **34**, 3077 (1986).
[8] L. A. Lugiato, M. O. Scully, and H. Walther, Phys. Rev. A **36**, 740 (1987).
[9] P. Meystre, in *Progress in Optics XXX*, edited by E. Wolf (Elsevier Science Publishers, New York, 1992), p. 261.
[10] J. M. Raimond, M. Brune, P. Goy, and S. Haroche, J. Phys. (Paris), Colloq. **15**, C-17 (1990).
[11] J. M. Raimond, M. Brune, L. Davidovich, P. Goy, and S. Haroche, in *Atomic Physics 11*, edited by S. Haroche, J. C. Gay, and G. Grynberg (World Scientific, Amsterdam, 1989), p. 441.
[12] P. Meystre and E. M. Wright, Phys. Rev. A **37**, 2524 (1988).
[13] G. Raithel, C. Wagner, H. Walther, L. M. Narducci, M. O. Scully, in *Cavity Quantum Electrodynamics*, edited by P. R. Berman (Academic Press, New York, 1994), p. 57.